

Article

N-Substituted (Hexahydro)-1*H*-isoindole-1,3(2*H*)-dione Derivatives: New Insights into Synthesis and Characterization

Carmellina Daniela Bădiceanu ^{1,†}, Catalina Mares ^{2,†}, Diana Camelia Nuță ^{1,*}, Speranța Avram ², Constantin Drăghici ³, Ana-Maria Udrea ^{4,5}, Irina Zarafu ⁶, Cornel Chiriță ⁷, Marilena Viorica Hovanet ⁸ and Carmen Limban ¹

¹ Department of Pharmaceutical Chemistry, Faculty of Pharmacy, “Carol Davila” University of Medicine and Pharmacy, 6 Traian Vuia, 020956 Bucharest, Romania; carmellina.badiceanu@umfcd.ro (C.D.B.); carmen.limban@umfcd.ro (C.L.)

² Department of Anatomy, Animal Physiology, and Biophysics, Faculty of Biology, University of Bucharest, 36-46 Bd. M. Kogalniceanu, 050107 Bucharest, Romania; catalina.sogor@gmail.com (C.M.); speranta.avram@gmail.com (S.A.)

³ “C. D. Nenitzescu” Institute of Organic and Supramolecular Chemistry, 202B Splaiul Independentei, 060023 Bucharest, Romania; cst_drag@yahoo.com

⁴ Laser Department, National Institute for Laser, Plasma and Radiation Physics, Atomistilor 409, 077125 Magurele, Romania; ana.udrea@inflpr.ro

⁵ Research Institute of the University of Bucharest—ICUB, University of Bucharest, 91-95 Splaiul Independentei, 050095 Bucharest, Romania

⁶ Department of Organic Chemistry, Biochemistry and Catalysis, Faculty of Chemistry, University of Bucharest, 4-12 Regina Elisabeta, 030018 Bucharest, Romania; irina.zarafu@chimie.unibuc.ro

⁷ Department of Pharmacology and Clinical Pharmacy, Faculty of Pharmacy, “Carol Davila” University of Medicine and Pharmacy, 6 Traian Vuia, 020956 Bucharest, Romania; cornel.chirita@umfcd.ro

⁸ Department of Pharmaceutical Botany and Cell Biology, Faculty of Pharmacy, “Carol Davila” University of Medicine and Pharmacy, 6 Traian Vuia, 020956 Bucharest, Romania; marilena.hovanet@umfcd.ro

* Correspondence: diana.nuta@umfcd.ro

† These authors contributed equally to this work.



Citation: Bădiceanu, C.D.; Mares, C.; Nuță, D.C.; Avram, S.; Drăghici, C.; Udrea, A.-M.; Zarafu, I.; Chiriță, C.; Hovanet, M.V.; Limban, C. N-Substituted (Hexahydro)-1*H*-isoindole-1,3(2*H*)-dione Derivatives: New Insights into Synthesis and Characterization. *Processes* **2023**, *11*, 1616. <https://doi.org/10.3390/pr11061616>

Academic Editors: Alina Pyka-Pająk, Francesca Raganati, Barbara Dolińska and Federica Raganati

Received: 27 April 2023

Revised: 22 May 2023

Accepted: 23 May 2023

Published: 25 May 2023



Copyright: © 2023 by the authors. Licensee MDPI, Basel, Switzerland. This article is an open access article distributed under the terms and conditions of the Creative Commons Attribution (CC BY) license (<https://creativecommons.org/licenses/by/4.0/>).

Abstract: Novel phthalimide derivatives, namely N-(1,3-dioxoisindolin-2-yl)-2-(2-methyl-4-oxoquinazolin-3(4*H*)-yl)acetamide (**1a**) and N-(1,3-dioxoisindolin-2-yl)thiophene-2-carboxamide (**1b**), and hexahydrophthalimide derivative N-(1,3-dioxohexahydro-1*H*-isoindol-2(3*H*)-yl)-2-(2-methyl-4-oxoquinazolin-3(4*H*)-yl)acetamide (**2**), have been synthesized. The phthalimide derivatives were synthesized from phthalic anhydride and 2-(2-methyl-4-oxoquinazolin-3(4*H*)-yl)acetohydrazide or thiophene-2-carbohydrazide, and the hexahydrophthalimide derivative has been synthesized from hexahydrophthalic anhydride and 2-(2-methyl-4-oxoquinazolin-3(4*H*)-yl)acetohydrazide. The chemical structures of the compounds are elucidated by Nuclear Magnetic Resonance (NMR) and Infrared (IR) spectra. The new in vitro antioxidant activities of the obtained substances were evaluated using the DPPH method. All tested compounds showed antioxidative activity, the most active compound being **1b**. Bioinformatics tools were used for the prediction of pharmacokinetics and pharmacodynamics profiles. Our results showed that all compounds have a suitable intestinal absorption rate, good BBB and CNS permeabilities and have as molecular targets MAO B, COX-2 and NF-κB, important for antioxidant activities.

Keywords: phthalimides; hexahydrophthalimides; anti-oxidant activity; pharmacokinetics and pharmacodynamic profiles; molecular docking

1. Introduction

Imides are used as intermediates in organic synthesis. Additionally, they can be structural moieties in biologically-active compounds such as drugs, fungicides, and herbicides [1].

Phthalimide (1*H*-isoindole-1,3(2*H*)-dione) serves as a compelling molecule in medicinal chemistry and is a privileged scaffold that can be utilized to create novel lead drug-candidates with diverse biological activities. Incorporation of the hydrophobic phthalimide moiety enhances the ability of compounds to traverse biological membranes *in vivo* [2].

Thalidomide ((*RS*)-2-(2,6-dioxopiperidin-3-yl)isoindole-1,3-dione) (Figure 1) is one of the compounds with phthalimide scaffold. The teratogenic effects observed in humans with thalidomide were attributed to the *S*-enantiomer, acting on protein Cereblon [3], whereas the *R*-enantiomer was found to induce sedative-hypnotic activities. Despite its association with teratogenicity [4], thalidomide has gained attention for its immunomodulatory and antiangiogenic properties and is currently used to treat certain cancers like multiple myeloma and complications of leprosy.

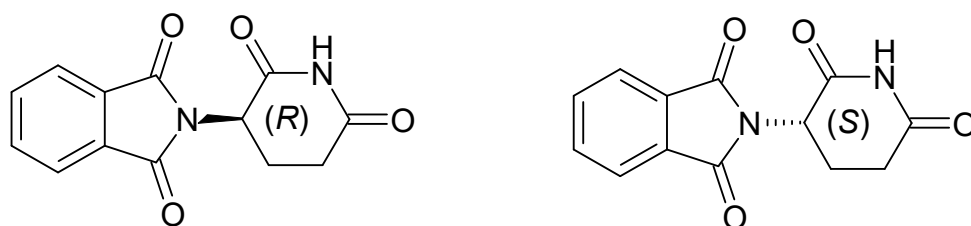


Figure 1. Thalidomide's chemical structure.

The quest for thalidomide analogs with improved safety profiles and enhanced immunomodulatory activity resulted in the development of lenalidomide and pomalidomide (Figure 2), which both contain an identical α -(isoindolinon-2-yl)-glutarimide core.

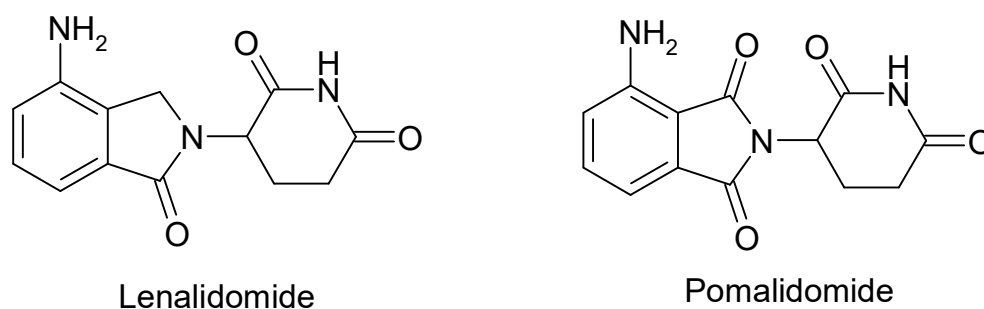


Figure 2. The chemical structure of lenalidomide and pomalidomide.

Pomalidomide, (4-amino-2-(2,6-dioxopiperidin-3-yl)isoindole-1,3-dione), exhibits antitumor effects, immunomodulatory and antiangiogenic properties, as well as direct antimyeloma activity when administered alongside low-dose dexamethasone. This compound exhibits a pleiotropic mechanism of action that aligns with the current cancer therapy approach, which focuses on inducing apoptosis in tumor cells, disrupting tumor interactions with the cellular microenvironment, and improving autoimmune responses [5].

N-substituted isoindoline-1,3-dione derivatives have garnered interest owing to their wide-ranging biological properties, such as antimicrobial [6,7], antitubercular [8], antiangiogenic [9], antitumor [10], antiviral [11], anticonvulsant [12], hypoglycemic [13], anti-inflammatory [14,15] and antioxidant [16] activities.

An aspect worthy of consideration is that of the condensation of acyl-hydrazides with phthalic anhydride or its derivatives, the subject being developed in research projects considering several therapeutic classes.

A group of researchers led by Fregnan conducted a study that involved synthesizing, characterizing, and assessing the antimicrobial properties of several derivatives of piparine, which is present in various species of *Piper*. The synthesis involved the obtaining of acyl-chlorides from cinnamic acid, 4-methoxycinnamic acid, 3,4-dimethoxycinnamic acid and 3,4,5-trimethoxycinnamic acid. The dichloromethane solutions of these acyl-

chlorides gave the corresponding acyl-hydrazides, used to obtain the new phthalimide derivatives (*E*)-*N*-(1,3-dioxoisindolin-2-yl)cinnamamide, (*E*)-*N*-(1,3-dioxoisindolin-2-yl)-3-(4-methoxyphenyl)acrylamide, (*E*)-3-(3,4-dimethoxyphenyl)-*N*-(1,3-dioxoisindolin-2-yl)acrylamide, and (*E*)-*N*-(1,3-dioxoisindolin-2-yl)-3-(3,4,5-trimethoxyphenyl)acrylamide. These compounds exhibit a moderate level of activity against various strains of fungi; the number of aromatic methoxy groups is important for their antifungal activity [17].

N-(1,3-dioxoisindolin-2-yl)-2-(4-oxo-3-phenyl-3,4-dihydroquinazolin-2-yl-thio)acetamide, having potential anti-inflammatory activity, was prepared from 2-thioxo-3-phenyl-quinazolin-4(3*H*)one with ethyl chloroacetate, after undergoing a reaction with hydrazine hydrate to afford the acyl-hydrazide; this derivative reacts with electrophilic reagent phthalic anhydride, in refluxing dioxane [18].

The ethyl ester derivative of 2,5-dimercapto-1,3,4-thiadiazole is formed by reacting 2,5-dimercapto-1,3,4-thiadiazole with ethyl bromoacetate in the presence of a base. The resulting product is then reacted with hydrazine hydrate to produce the corresponding carbohydrazide. The hydrazide is subsequently treated with different anhydrides, such as succinic, maleic, and phthalic anhydrides, under the same conditions (reflux for 10 h in acetic acid) to generate novel derivatives of 2,5-disubstituted-1,3,4-thiadiazole with tetrahydro-3,6-pyridazinedione, pyrroline-2,5-dione, and isoindole-1,3-dione moieties, respectively [19].

Al-Omran et al., reported, in an article from 2016, the synthesis of 2-(benzo[d]thiazol-2'-ylthio)-*N'*-(1,3-dioxoisindolin-2-yl)acetamide by the refluxing of 2-(benzo[d]thiazol-2'-ylthio)acetohydrazide with a solution in acetic acid of phthalic anhydride [20].

Kaur et al., utilized a comparable approach to synthesize *N*-(1,3-dioxoisindolin-2-yl)-1-(substituted-phenyl)-1*H*-1,2,3-triazole-4-carboxamide. The reaction involved 1-(substituted-phenyl)-1*H*-1,2,3-triazole-4-carbohydrazide, phthalic anhydride, and a catalytic amount of glacial acetic acid in toluene, and was carried out at 110 °C [21].

On the other hand, among the widely used components in the field of pesticide chemistry are hexahydrophthalimides, such as flumiclorac-pentyl, cinidon-ethyl, and flumioxazin, which act as protoporphyrinogen oxidase inhibitors [22].

It has been shown in several studies that molecules containing a phthalimide or hexahydrophthalimide structure can serve as a framework for developing novel antioxidant compounds [23].

The quinazoline and thiophene nuclei improve the biological activity of some molecules, including the antioxidant activity, making them attractive preventive agents in various oxidative diseases, like neurovascular, cardiovascular, and autoimmune diseases [24–27].

Substituted 2-(4-oxoquinazolin-3(4*H*)-yl)acetamide derivatives were synthesized and tested as novel enoyl-acyl carrier protein reductase (InhA) inhibitors for the treatment of tuberculosis, with 2-(6-chloro-2-methyl-4-oxoquinazolin-3(4*H*)-yl)-*N*-phenylacetamide being the most active compound [28]. Additionally, *N*-(substituted-phenyl)-2-(4-oxoquinazolin-3(4*H*)-yl)acetamide derivatives were tested as *Mycobacterium tuberculosis* bd oxidase inhibitors [29].

The biological activity of thiophene-2-carboxamide derivatives is well established. Derivatives 5-cyano-*N*-(4-methoxyphenyl)-2-phenylamino-4-(2-arylamino-acetamido) thiophene-3-carboxamides were investigated for their potential as dual anti-angiogenesis and antimetabolic agents. The *in vitro* anti-proliferative activity of these compounds against gastrointestinal solid cancer cell lines (HepG-2 and HCT-116) was also studied [30].

Based on this evidence, and aiming to obtain new antioxidant agents, we designed, and synthesized new derivatives of 1*H*-isoindole-1,3(2*H*)-dione and hexahydro-1*H*-isoindole-1,3(2*H*)-dione connected to 2-methyl-4-oxoquinazolin and thiophene moieties via a hydrazide linkage.

Using the molecular docking approach, we calculated the binding affinities of *N*-(1,3-dioxoisindolin-2-yl)-2-(2-methyl-4-oxoquinazolin-3(4*H*)-yl)acetamide (**1a**), *N*-(1,3-dioxoisindolin-2-yl)thiophene-2-carboxamide (**1b**), and *N*-(1,3-dioxohexahydro-1*H*-isoindol-2(3*H*)-yl)-2-(2-methyl-4-oxoquinazolin-3(4*H*)-yl)acetamide (**2**), when interacting with hu-

man Monoamine Oxidase B (MAO-B), Cyclooxygenase-2 (COX-2) and Nuclear Factor Kappa B (NF-KB).

2. Materials and Methods

2.1. General Information

The compounds' synthesis employed reagents and solvents sourced from Merck Schuchardt, in Hohenbrunn, Germany, MP Biomedicals LLC in Eschwege, Germany, and Sigma-Aldrich in Steinheim, Germany.

2.2. Measurement

The reported physical and spectroscopic data are crucial for confirming the identity and purity of the synthesized compounds and provide valuable insights into their chemical and physical properties.

An Electrothermal 9100 melting point apparatus (Bibby Scientific Ltd, Stone, UK) was used to determine the melting points (uncorrected) of synthesized compounds.

The Bruker Vertex 70 FT-IR spectrometer (Bruker Corporation, Billerica, MA, USA) was used to obtain the IR spectra of the compounds. The signal intensities were represented using the abbreviations: w—for weak, m—for medium, s—for intense, and vs—for very intense.

The Varian Gemini 300BB instrument (Varian Medical Systems, Palo Alto, CA, USA) was utilized to conduct the nuclear magnetic resonance (NMR) spectra measurements, with 300 MHz for proton (^1H) NMR and 75 MHz for carbon-13 (^{13}C) NMR.

The chemical shifts were expressed in parts per million (δ , ppm) and referenced to tetramethylsilane (TMS), $(\text{CH}_3)_4\text{Si}$, which served as an internal standard. The solvent used was DMSO- d_6 , and the coupling constants (J) were reported in Hertz (Hz). The ^1H multiplicities were abbreviated as follows: singlet (s), broad singlet (brs), broad doublet (brd), broad triplet (brt), doublet of doublets (dd), triple doublet (td), and multiplet (m).

In reporting the data, the order is as follows: chemical shifts, multiplicity, coupling constants, number of protons, and signal/atom attribution. For the ^{13}C NMR data, the order is chemical shifts and signal/atom attribution. Quaternary carbon atoms are designated as "q".

2.3. Chemical Synthesis

We treated a solution obtained by solubilizing 2-(2-methyl-4-oxoquinazolin-3(4H)-yl)-acetohydrazide (0.01 moles) (Mw 232.0 g/mol) or 2-thiophenecarboxylic acid hydrazide (0.01 moles) (Mw 142.18 g/mol) in 150 mL glacial acetic acid with a solution resulting from the dissolution of phthalic anhydride (0.01 moles) (Mw 148.1 g/mol) in 150 mL glacial acetic acid. The reaction mixture is stirred and refluxed for a duration of 5 h. After cooling, it is poured into 500 mL of ice water when N-(1,3-dioxoisindolin-2-yl)-2-(2-methyl-4-oxoquinazolin-3(4H)-yl)acetamide or, respectively, N-(1,3-dioxoisindolin-2-yl)thiophene-2-carboxamides precipitates, are filtered off. The purification process involved recrystallization with animal charcoal, using either isopropyl alcohol or ethyl alcohol.

In order to synthesize N-(1,3-dioxohexahydro-1H-isoindol-2(3H)-yl)-2-(2-methyl-4-oxoquinazolin-3(4H)-yl)acetamide, 2-(2-methyl-4-oxoquinazolin-3(4H)-yl)acetohydrazide (0.00125 mol) (Mw 232.0 g/mol) is dissolved in 150 mL glacial acetic acid and is treated with tetrahydrophthalic anhydride (0.00125 mol; Mw 152.14 g/mol) in 150 mL of glacial acetic acid; stirring and refluxing are applied for 5 h. Once cooled, the resulting mixture is poured into 500 mL of ice water, which causes the crude compound to precipitate. The mixture is then filtered and recrystallization from ethyl alcohol, in the presence of charcoal, was performed to obtain the pure compound.

2.4. Anti-Oxidant Activity

In this study, we employed the 2,2-diphenyl-1-picrylhydrazyl (DPPH) method [31–33] to measure the total antioxidant activity (TAC %). Although various methods are available

in the literature for TAC measurement, we chose the DPPH method. The DPPH solution was prepared in methanol at a concentration of 0.2 mmol, and the test compounds were dissolved in the same solvent at a concentration of 0.5 mg/mL. To evaluate TAC, 1.8 mL of the DPPH solution was mixed with 0.2 mL of each compound solution and kept in the dark (a control test was performed using 1.8 mL of DPPH solution and 0.2 mL of methanol). After 30 min, the absorbance of the solutions was measured at 517 nm, and TAC values were calculated using the following equation.

$$TAC(\%) = \frac{Abs\ 0 - Abs\ 30\ min}{Abs\ 0} \times 100$$

where *Abs 0* represents the initial absorption of the DPPH solution and *Abs 30 min* represents the absorbance of the mixture of DPPH and the corresponding compound after 30 min. Ascorbic acid was used as the antioxidant reference.

2.5. Molecular Modeling

1a, **1b**, and **2** derivatives were 3D protonated, and the energy was minimised using a force field with a gradient of 0.05 and the Gasteiger partial charges. For the minimisation protocol, we have used Molecular Operating Environment software (MOE ver 2018; Chemical Computing Group; Montreal, Canada) [34].

From the Protein Data Bank (PDB) [35], we imported the 3D structures of MAO-B (PDB ID 1GOS) [36], COX-2 (PDB ID 5KIR) [37], and NF-KB (PDB ID 1SCV) [38]. The structures were optimized for molecular docking by applying our usual protocol [39,40].

Besides, the Simplified Molecular Input Line Entry (SMILES) file of compounds was obtained by using Molecular Operating Environment (MOE) software [41,42] and used for further pharmacokinetics analyses.

2.5.1. Molecular Docking

Autodock 4.2.6 software [43] was used for the molecular docking analysis. We employed the same protocol as in our previous studies to predict the interaction between the derivatives and molecular targets [44,45].

2.5.2. Computational Pharmacokinetics (ADME-Tox)

To study the potential chemical structure–biological relationship of compounds **1a**, **1b** and **2** [46], the SMILES files were downloaded into pkCSM database [47] to examine absorption, distribution, metabolism, and excretion properties (ADME). From all of the pharmacokinetic items available in the database, the following were selected: Human Intestinal Absorption, Skin Permeability, Blood–Brain Barrier/CNS Barrier, Plasma Protein Binding, primarily renal uptake transporter (OCT2) inhibitors, and toxicity items such as AMES toxicity, hERG I/II inhibitors, Oral Rat Acute Toxicity (LD50), Hepatotoxicity, and Skin Sensitization.

2.5.3. Computational Pharmacodynamic Profiles of Compounds

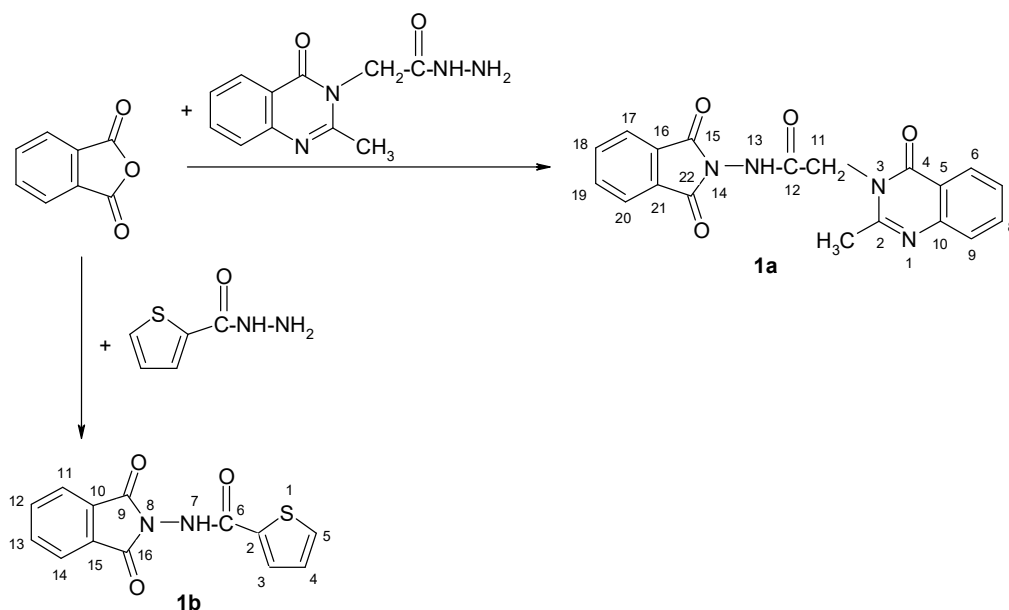
The chemical structure–molecular targets [48] relationships of compounds **1a**, **1b** and **2** were predicted by SuperPred database [49]. SuperPred is a prediction web server for small molecule targets, thus providing information about chemical compounds. The database was built with the help of automatic learning models of logical regression. The choice of this tool is given by the two scores obtained in predicting the molecular target, namely the “probability” which refers to the probability that the searched structure will attach to the specific target and the “accuracy of the model” where the 10-fold cross-validation score of the model is displayed of logistic regression respectively [50].

The binding data and resulting model accuracy used in this study were based on a dataset of 646 human targets. The molecular docking analysis was performed on these targets to predict the binding affinity and mode of interaction between the compounds and the targets. The therapeutic indications of the predicted targets were also identified

based on their relevance to the therapeutic indications of the compounds. These results provide valuable insights into the potential pharmacological effects of the compounds and can guide further experimental studies to validate the predicted targets and their associated therapeutic indications.

3. Results

The new phthalimide-2-methyl-4-oxo-4*H*-quinazoline and phthalimide-thiophene hybrids were obtained according with Scheme 1.



Scheme 1. The synthesis of the new 1*H*-isoindole-1,3(2*H*)-dione derivatives **1a** and **1b**.

Compound 1a: N-(1,3-dioxoisindolin-2-yl)-2-(2-methyl-4-oxoquinazolin-3(4*H*)-yl)acetamide; m.p. 305–307 °C; yield 67%.

¹H-NMR (DMSO-*d*₆, δ ppm, J Hz): 11.30 (s, 1H, H-13); 8.11 (brd, 8.0, 1H, H-6); 7.90–8.00 (m, 4H, H-17, H-18, H-19, H-20); 7.81 (td, 8.0, 1.4, 1H, H-8); 7.60 (brd, 8.0, 1H, H-9); 7.50 (br d, 8.0, 1H, H-7); 5.10 (s, 2H, H-11); 2.57 (s, 3H, -CH₃).

¹³C-NMR (DMSO-*d*₆, δ ppm): 166.79 (C-12); 164.85 (C-15, C-22); 161.06 (C-4); 154.92 (C-2); 146.98 (C-10); 135.36 (C-17, C-20); 134.67 (C-6); 129.37 (Cq); 126.62 (CH); 126.55 (CH); 126.32 (CH); 123.84 (C-18, C-19); 119.54 (C-5); 44.41 (C-11); 22.65 (-CH₃).

FT-IR (solid in ATR, ν cm⁻¹): 3102w; 2826w; 2361w; 2206w; 2037w; 1794w; 1739vs; 1676vs; 1599vs; 1523m; 1470s; 1385s; 1223s; 1119m; 955m; 878m; 697s.

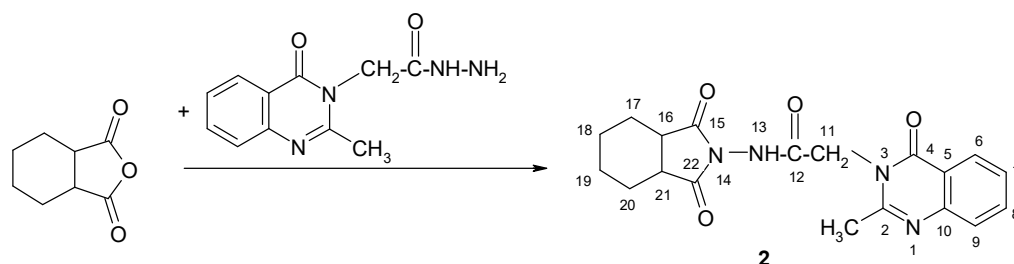
Compound 1b: N-(1,3-dioxoisindol-2-yl)thiophene-2-carboxamide; m.p. 99–102 °C; yield 79%.

¹H-NMR (DMSO-*d*₆, δ ppm, J Hz): 8.48 (s, 1H, NH-7); 7.85 (dd, 5.5, 3.5, 2H, H-11, H-14); 7.73 (dd, 5.5, 3.5, 2H, H-12, H-13); 7.66 (dd, 3.9, 1.1, 1H, H-3); 7.48 (dd, 4.9, 1.1, 1H, H-5); 7.02 (dd, 4.9, 3.9, 1H, H-4).

¹³C-NMR (DMSO-*d*₆, δ ppm): 166.17 (C-9; C-16); 161.12 (C-6); 136.32 (C-11, C-14); 135.86 (C-2); 134.07 (C-10, C-15); 131.44 (C-5); 130.21 (C-3); 129.41 (C-4); 124.78 (C-12, C-13).

FT-IR (solid in ATR, ν cm⁻¹): 3491m; 3400w; 3158w; 3081w; 2997w; 2847w; 1788m; 1707vs; 1651vs; 1554m; 1461w; 1416m; 1353m; 1297s; 1204m; 1124m; 1078m; 980w; 884m; 791s; 580m.

The method described in Scheme 2 was applied in order to obtain the hexahydrophthalimide-2-methyl-4-oxo-4*H*-quinazoline hybrid.



Scheme 2. The synthesis of the new hexahydro-1H-isoindole-1,3(2H)-dione derivative **2**.

Compound 2: N-(1,3-dioxohexahydro-1H-isoindol-2(3H)-yl)-2-(2-methyl-4-oxoquinazolin-3(4H)-yl)acetamide; m.p. 283.5–286 °C; yield 74%.

¹H-NMR (DMSO-d₆, δ ppm, J Hz): 11.08 (s, 1H, NH-13); 8.10 (brd, 8.0; 1H, H-6); 7.81 (td, 8.0, 1.7, 1H, H-8); 7.61 (brd, 8.0, 1H, H-9); 7.50 (brt, 8.0, 1H, H-7); 5.02 (s, 2H, H-11); 3.07 (m, 2H, H-16, 21); 1.20–1.80 (m, 8H, H-17, H-18, H-19, H-20); 2.45 (s, 3H, -CH₃).

¹³C-NMR (DMSO-d₆, δ ppm): 176.19 (C-15, C-22); 166.09 (C-12); 161.02 (C-4); 154.89 (C-2); 146.97 (C-10); 134.62 (C-6); 126.58 (CH); 126.49 (C-7); 126.28 (C-8); 119.54 (C-5); 44.33 (C-11); 37.38 (C-16, C-21); 23.21 (-CH₂-); 22.61 (-CH₃); 21.13 (-CH₂-).

FT-IR (solid in ATR, ν cm⁻¹): 3432w; 2856m; 2355w; 2224w; 2037w; 1781w; 1680vs; 1600s; 1560m; 1475m; 1397m; 1198s; 1096w; 962w; 886w; 693w.

The spectra are presented in the Supplementary Materials files (Figures S1–S9 from Supplementary Materials).

3.1. Total Antioxidant Capacity (TAC) Measurements

Antioxidant activity is an important property used to characterize biologically-active substances, as it is associated with their ability to shield living cells from the detrimental effects of free radicals. The results obtained for the three compounds tested were 25.88%, 31.45%, and 25.99%, respectively.

The predicted interactions between the derivatives and molecular targets concerning the antioxidant activity of **1a**, **1b**, and **2** derivatives are presented in Table 1.

Table 1. Predicted interactions between protein targets for antioxidant activity and the **1a**, **1b**, and **2** derivatives. The lower the estimated free energy of binding, the higher the chance that the compound will bind to the specific target.

Compound	1a	1b	2
NF-KB	−8.29 kcal/mol	−8.13 kcal/mol	−7.98 kcal/mol
COX-2	−8.55 kcal/mol	−10.58 kcal/mol	−10.44 kcal/mol
MAO-B	−8.69 kcal/mol	−10.70 kcal/mol	−10.62 kcal/mol

The results obtained after predicting the interaction between the target proteins and the analyzed compounds represent the free binding energy. The more negative the value of the binding energy, the more complex the link of the complex formed between the macromolecule (target) and the ligand.

Compound **1b** forms conventional hydrogen bond interactions with amino acid (AA) residues GLY 434 and MET 436 of MAO-B (Figure 3). The interactions between the rest of the compounds and NF-KB, COX-2, and MAO-B are presented in the Supplementary Materials files (Figures S10–S17 from Supplementary Materials).

The structure of MAO-B was co-crystallized with the flavin-adenine dinucleotide compound. The experimentally-determined interaction between flavin-adenine dinucleotide and MAO-B (Figure 4) shows a similar interaction site to the predicted interaction between MAO-B and **1b** (Figure 3).

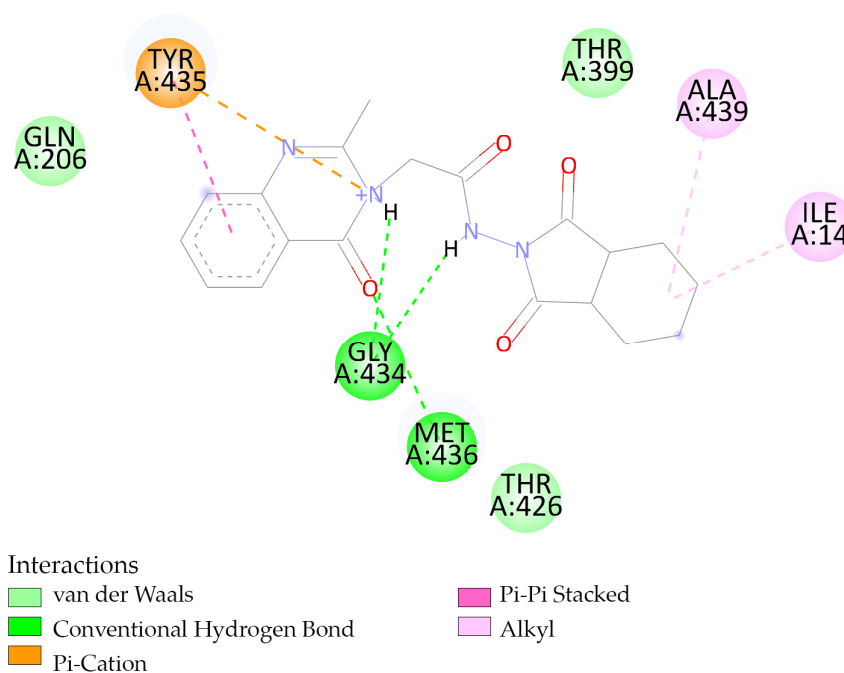


Figure 3. Interactions between **1b** and MAO-B.

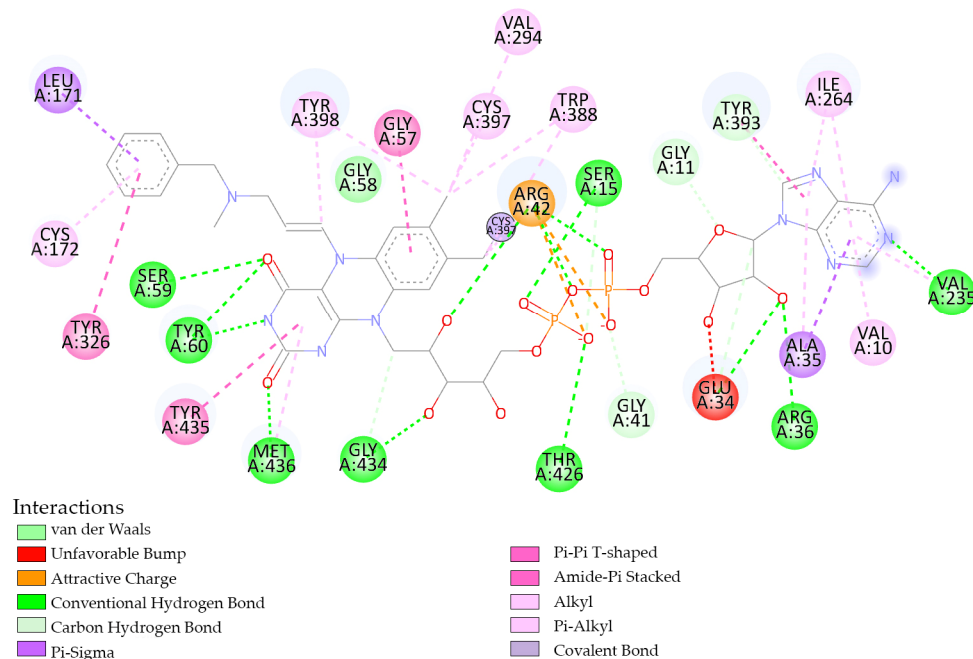


Figure 4. Experimental obtained interaction between flavin-adenine dinucleotide and MAO-B (PDB ID: 1GOS) [36].

3.2. Pharmacokinetics and Pharmacodynamics Profiles

Hepatotoxicity represents an acute or chronic side effect in the liver tissue that can be caused by drugs, natural compounds, chemicals, solvents. It is important to evaluate the effect of these compounds on the liver because it is the main site of drug metabolism. At the same time, these predictions help us to analyze, based on the algorithms, the potential risk-benefit ratio of the analyzed compounds. The symptoms can be observed quickly, being represented by fatigue, feeling sick, yellow skin and eyes, palmar erythema [50].

Table 2 summarizes the evaluation of the ADME-predictable properties of the **1a**, **1b**, and **2** compounds, including their kinetic characteristics such as human intestinal

absorption, skin permeability, fraction unbound in human plasma, permeabilities across the blood-brain barrier and central nervous system, renal OCT2 substrate, and toxicities.

Table 2. Computational pharmacokinetics profiles for compounds **1a**, **1b** and **2**.

Pharmacokinetics	Compound 1a	Compound 1b	Compound 2
Intestinal absorption (human) %	82.55	77.103	78.181
Skin Permeability (log Kp)	−3.778	−3.104	−2.925
Fraction unbound (human) (Fu)	0.358	0.474	0.286
BBB permeability (logBBB)	−0.129	−0.422	−0.463
CNS permeability (logPS)	−2.953	−2.76	−2.851
Renal OCT2 substrate	NO	NO	NO
AMES toxicity	NO	NO	NO
hERG I/II inhibitor	NO	NO	NO/YES
Hepatotoxicity	NO	YES	YES
Skin Sensitisation	NO	NO	NO
Oral Rat Acute Toxicity (LD50) (mol/kg)	2.425	2.451	1.878

Regarding the predicted interactions of compounds with molecular targets our results revealed that the compounds have as targets—Nuclear factor NF-kappa-B, Cyclooxygenase-2 and Monoamine oxidase A (Table 3).

Table 3. The predicted interactions of compounds with molecular targets.

Targets	Compound 1a Binding Probability/ Model Accuracy	Compound 1b Binding Probability/ Model Accuracy	Compound 2 Binding Probability/ Model Accuracy
Nuclear factor NF-kappa-B	85.47/ 96.09	93.29%/ 96.09%	89.59%/ 96.09%
Cyclooxygenase-2	90.77/ 89.63	-	81.17%/ 89.63%
Monoamine oxidase	-	-	56.98%/ 91.49%

4. Discussion

Having the experience of our group in synthesis of quinazoline and thiophene derivatives, we present in this paper an efficient and rapid method (Schemes 1 and 2) to obtain new (hexahydro)phthalimide-2-methyl-4-oxo-4H-quinazoline hybrids (novel substances) and a phthalimide-thiophene hybrid, by refluxing a mixture of different hydrazides with phthalic anhydride or tetrahydrophthalic anhydride for 5h in acetic acid glacial.

The process of obtaining 2-(2-methyl-4-oxoquinazolin-3(4H)-yl)-acetohydrazide has been previously described [51].

Antioxidant activity is a significant property that characterizes biologically-active substances, as it is closely related to their ability to safeguard living cells against the harm induced by free radicals. The compounds **1a** and **2** have quite similar activity, while **1b** showed an increased antioxidant character. This can be correlated with the chemical structure that contains a thiophene moiety, being known that compounds containing sulfur have a significant antioxidant activity.

The lower the predicted binding energy, the higher the probability that the compound will bind to that target. Our results indicate that the lower result is obtained when **1b** interacts with MAO-B (Table 1). However, low predicted results were also obtained when **1b** interacts with COX-2 and when **2** interacts with COX-2 and MAO-B (Table 1).

Our results showed that the lowest binding energies between our compounds and target proteins were obtained when they interacted with MAO-B (Table 1).

Compound **1b** forms conventional hydrogen bond interactions with amino acid (AA) residues GLY 434 and MET 436 of MAO-B (Figure 3).

Flavin-adenine dinucleotide and **1b** have four interactions in common with AA residues from MAO-B. They both form conventional hydrogen bond interactions with the AA residues GLY434 and MET436 (Figures 3 and 4). When it interacts with THR426 flavin-adenine dinucleotide, it forms a conventional hydrogen bond, while **1b** forms weak intermolecular forces, respectively van der Waals interactions (Figures 3 and 4). When interacting with TYR435, **1b** forms a Pi-cation and a Pi-Pi stacked, and flavin-adenine dinucleotide forms a Pi-Pi T-shaped interaction (Figures 3 and 4).

Our predicted results showed that all three compounds may have middle intestinal absorption properties but these compounds presented very appropriate permeabilities at the nervous system and brain-blood barrier.

5. Conclusions

Our strategy was to generate derivatives containing 2-methyl-4-oxo-4*H*-quinazoline and thiophene moiety connected to 1*H*-isoindole-1,3(2*H*)-dione or hexahydro-1*H*-isoindole-1,3(2*H*)-dione. All tested compounds showed antioxidant activity. It is noteworthy that this is more evident for the derivative containing a thiophene moiety.

Our molecular docking simulations have revealed derivatives **1b** and **2** that exhibit a low binding energy while interacting with COX-2 and MAO-B. A low predicted energy of binding is related to a high probability of interaction between the compound and the target. Regarding the pharmacokinetic profiles, all three compounds are good candidates for antioxidant activity. It must be noted that the predicted non-toxic features of compounds and suitable BBB permeability and CNS permeability features should be considered for future in vitro studies.

Supplementary Materials: The following supporting information can be downloaded at: <https://www.mdpi.com/article/10.3390/pr11061616/s1>. Figure S1: The 1H-NMR spectra of N-(1,3-dioxohexahydro-1*H*-isoindol-2(3*H*)-yl)-2-(2-methyl-4-oxoquinazolin-3(4*H*)-yl)acetamide; Figure S2: The 13C-NMR spectra of N-(1,3-dioxohexahydro-1*H*-isoindol-2(3*H*)-yl)-2-(2-methyl-4-oxoquinazolin-3(4*H*)-yl)acetamide; Figure S3: The FT-IR spectra of N-(1,3-dioxohexahydro-1*H*-isoindol-2(3*H*)-yl)-2-(2-methyl-4-oxoquinazolin-3(4*H*)-yl)acetamide; Figure S4: The 1H-NMR spectra of N-(1,3-dioxoisindolin-2-yl)-2-(2-methyl-4-oxoquinazolin-3(4*H*)-yl)acetamide; Figure S5: The 13C-NMR spectra of N-(1,3-dioxoisindolin-2-yl)-2-(2-methyl-4-oxoquinazolin-3(4*H*)-yl)acetamide; Figure S6: The FT-IR spectra of N-(1,3-dioxoisindolin-2-yl)-2-(2-methyl-4-oxoquinazolin-3(4*H*)-yl)acetamide; Figure S7: The 1H-NMR spectra of N-(1,3-dioxoisindol-2-yl)thiophene-2-carboxamide; Figure S8: The 13C-NMR spectra of N-(1,3-dioxoisindol-2-yl)thiophene-2-carboxamide; Figure S9: The FT-IR spectra of N-(1,3-dioxoisindol-2-yl)thiophene-2-carboxamide; Figure S10: The 2D interaction between NF-KB and compound 1a; Figure S11: The 2D interaction between NF-KB and compound 1b; Figure S12: Interaction between NF-KB and compound 2; Figure S13: Interaction between COX-2 and compound 1a; Figure S14: Interaction between COX-2 and compound 1b; Figure S15: Interaction between COX-2 and compound 2; Figure S16: Interaction between MAO-B and compound 1a; Figure S17: Interaction between MAO-B and compound 2.

Author Contributions: Conceptualization, C.D.B. and C.M.; methodology, C.D.B., C.M., S.A., C.D. and I.Z.; software, C.M., S.A. and A.-M.U.; validation, D.C.N., C.L., I.Z., C.D. and S.A.; formal analysis, A.-M.U., C.C. and M.V.H.; investigation, C.D.B., C.M., D.C.N., S.A., C.D., A.-M.U., I.Z., C.C., M.V.H. and C.L.; resources, C.M. and S.A.; data curation C.M. and S.A.; writing—original draft preparation, D.C.N., S.A., C.C. and C.L.; writing—review and editing, D.C.N., S.A. and C.L.; visualization, C.D.B.; supervision, C.D. and S.A.; project administration, C.D.B. and C.M.; funding acquisition, D.C.N. and S.A. All authors have read and agreed to the published version of the manuscript.

Funding: This research was funded by the Ministry of Research, Innovation and Digitization, CNCS-UEFISCDI; project number PN-III-P1-1.1-PD-2021-0225, Nucleu Program LAPLAS VII—contract no. 30N/2023, project numbers PN-III-P2-2.1-PED-2021-2866. Publication of this paper was supported by the University of Medicine and Pharmacy Carol Davila, through the institutional program Publish not Perish.

Data Availability Statement: Not applicable.

Conflicts of Interest: The authors declare no conflict of interest.

References

1. Benz, G. *Synthesis of Amides and Related Compounds*; Comprehensive Organic Synthesis; Pergamon Press: Oxford, UK, 1991; Volume 6, pp. 381–417.
2. Bansode, T.N.; Shelke, J.V.; Dongre, V.G. Synthesis and antimicrobial activity of some new N-acyl substituted phenothiazines. *Eur. J. Med. Chem.* **2009**, *44*, 5094–5098. [[CrossRef](#)] [[PubMed](#)]
3. Wang, M.; Dimopoulos, M.A.; Chen, C.; Cibeira, M.T.; Attal, M.; Spencer, A.; Rajkumar, S.V.; Yu, Z.; Olesnyckyj, M.; Zeldis, J.B.; et al. Lenalidomide plus dexamethasone is more effective than dexamethasone alone in patients with relapsed or refractory multiple myeloma regardless of prior thalidomide exposure. *Blood* **2008**, *112*, 4445–4451. [[CrossRef](#)] [[PubMed](#)]
4. Chang, X.; Zhu, Y.; Shi, C.; Stewart, A.K. Mechanism of immunomodulatory drugs' action in the treatment of multiple myeloma. *Acta Biochim. Biophys. Sin.* **2014**, *46*, 240–253. [[CrossRef](#)] [[PubMed](#)]
5. Ruchelman, A.L.; Man, H.W.; Zhang, W.; Chen, R.; Capone, L.; Kang, J.; Parton, A.; Corral, L.; Schafer, P.H.; Darius, B.; et al. Isosteric analogs of lenalidomide and pomalidomide: Synthesis and biological activity. *Bioorg. Med. Chem. Lett.* **2013**, *23*, 360–365. [[CrossRef](#)] [[PubMed](#)]
6. Khidre, R.E.; Abu-Hashem, A.A.; El-Shazly, M. Synthesis and anti-microbial activity of some 1-substituted amino-4,6-dimethyl-2-oxo-pyridine-3-carbonitrile derivatives. *Eur. J. Med. Chem.* **2011**, *46*, 5057–5064. [[CrossRef](#)] [[PubMed](#)]
7. Sabastiyan, A.; YosuvaSuvaikin, M. Synthesis, characterization and antimicrobial activity of 2-(dimethylaminomethyl)isoindoline-1,3-dione and its cobalt (II) and nickel (II) complexes. *Adv. Appl. Sci. Res.* **2012**, *3*, 45–50.
8. Santos, J.L.; Yamasaki, P.R.; Chin, C.M.; Takashi, C.H.; Pavan, F.R.; Leite, C.Q. Synthesis and in vitro anti mycobacterium tuberculosis activity of a series of phthalimide derivatives. *Bioorg. Med. Chem.* **2009**, *17*, 173795–173799. [[CrossRef](#)]
9. Noguchi, T.; Fujimoto, H.; Sano, H.; Miyajima, A.; Miyachi, H.; Hashimoto, Y. Angiogenesis inhibitors derived from thalidomide. *Bioorg. Med. Chem. Lett.* **2005**, *15*, 5509–5513. [[CrossRef](#)]
10. Chan, S.H.; Lam, K.H.; Chui, C.H.; Gambari, R.; Yuen, M.C.; Wong, R.S.; Cheng, G.Y.; Lau, F.Y.; Au, Y.K.; Cheng, C.H.; et al. The preparation and in vitro antiproliferative activity of phthalimide based ketones on MDAMB-231 and SKHep-1 human carcinoma cell lines. *Eur. J. Med. Chem.* **2009**, *44*, 2736–2740. [[CrossRef](#)]
11. Yang, Y.J.; Zhao, J.H.; Pan, X.D.; Zhang, P.C. Synthesis and antiviral activity of phthiobuzone analogues. *Chem. Pharm. Bull.* **2010**, *58*, 208–211. [[CrossRef](#)]
12. Kathuria, V.; Pathak, D.P. Synthesis and anticonvulsant activity of some N-substituted phthalimide analogues. *Pharm. Innov. J.* **2012**, *1*, 55–59. [[CrossRef](#)]
13. Mbarki, S.; Elhallaoui, M. 3D-QSAR for α -glucosidase inhibitory activity of N-(phenoxyalkyl) phthalimide derivatives. *Int. J. Recent. Res. Appl. Stud.* **2012**, *11*, 395–401.
14. Lima, L.M.; Castro, P.; Machado, A.L.; Fraga, C.A.; Lugnier, C.; de Moraes, V.L.; Barreiro, E.J. Synthesis and antiinflammatory activity of phthalimide derivatives, designed as new thalidomide analogues. *Bioorg. Med. Chem.* **2002**, *10*, 3067–3073. [[CrossRef](#)] [[PubMed](#)]
15. Sharma, U.; Kumar, P.; Kumar, N.; Singh, B. Recent advances in the chemistry of phthalimide analogues and their therapeutic potential. *Mini Rev. Med. Chem.* **2010**, *10*, 678–704. [[CrossRef](#)]
16. Karthik, C.S.; Mallesha, L.; Mallu, P. Investigation of antioxidant properties of phthalimide derivatives. *Can. Chem. Trans.* **2015**, *3*, 199–206. [[CrossRef](#)]
17. Fregnan, A.M.; Brancaglioni, G.A.; Galvão, A.F.C.; D'Sousa Costa, C.O.; Moreira, D.R.M.; Soares, M.B.P.; Bezerra, D.P.; Silva, N.C.; de Souza Moraes, S.M.; Oliver, J.Q.; et al. Synthesis of pipartine analogs and preliminary findings on structure–antimicrobial activity relationship. *Med. Chem. Res.* **2017**, *26*, 603–614. [[CrossRef](#)]
18. Mahmoud, R.M.; Abou-Elmagd, W.S.I.; Abdelwahab, S.S.; Soliman, E.-S.A. Synthesis and Spectral Characterization of Novel 2,3-Disubstituted Quinazolin-4(3H) one Derivatives. *Am. J. Org. Chem.* **2012**, *2*, 1–8. [[CrossRef](#)]
19. Awad, S.; Hussein, A.; Razzak, A.; Kubba, M. Synthesis, characterization and antimicrobial activity of new 2,5-disubstituted-1,3,4-thiadiazole derivatives. *Der Pharm. Chem.* **2015**, *7*, 250–260.
20. Al-Omran, F.; El-Khair, A.A. Synthesis, Spectroscopy and X-Ray Characterization, of Novel Derivatives of Substituted 2-(Benzothiazol-2'-ylthio)acetohydrazide. *Int. J. Org. Chem.* **2016**, *6*, 31–43.
21. Kaur, R.; Singh, R.; Kumar, A.; Singh, K. Click Chemistry Approach to Isoindole-1,3-dione Tethered 1,2,3-Triazole Derivatives. *SynOpen* **2019**, *3*, 67–70. [[CrossRef](#)]
22. Wu, Q.Y.; Jiang, L.L.; Yang, S.G.; Zuo, Y.; Wang, Z.F.; Xi, Z.; Yang, G.F. Hexahydrophthalimide–benzothiazole hybrids as a new class of protoporphyrinogen oxidase inhibitors: Synthesis, structure–activity relationship, and DFT calculations. *New J. Chem.* **2014**, *38*, 4510–4518. [[CrossRef](#)]
23. Lamie, P.F.; Philoppes, J.N.; El-Gendy, A.O.; Rarova, L.; Gruz, J. Design, Synthesis and Evaluation of Novel Phthalimide Derivatives as in Vitro Anti-Microbial, Anti-Oxidant and Anti-Inflammatory Agents. *Molecules* **2015**, *20*, 16620–16642. [[CrossRef](#)]
24. Teter, Z.; Zicane, D.; Ravina, I.; Mierina, I.; Rijkure, I. Synthesis and Antioxidant Properties of Novel Quinazoline Derivatives. *Mater. Sci. App. Chem.* **2014**, *30*, 51–54. [[CrossRef](#)]
25. Konus, M.; Algso, M.; Yilmaz, C.; Khorsheed, B.A.; Köroğlu, A.; Çetin, D.; Ergin, D.; Kivrak, A. Synthesis of Ethynyl-Thiophene Derivatives, Antioxidant Properties and ADME Analysis. *Chem. Sel.* **2022**, *7*, e2022002. [[CrossRef](#)]

26. Mehdhar, F.S.; Abdel-Galil, E.; Saeed, A.; Abdel-Latif, E.; Abd El Ghani, G.E. Synthesis of New Substituted Thiophene Derivatives and Evaluating their Antibacterial and Antioxidant Activities. *Polycycl. Aromat. Compd.* **2022**, 1–16. [[CrossRef](#)]
27. Mishra, R.; Kumar, N.; Sachan, N. Thiophene and Its Analogs as Prospective Antioxidant Agents: A Retrospective Study. *Mini Rev. Med. Chem.* **2022**, *22*, 1420–1437. [[CrossRef](#)] [[PubMed](#)]
28. Pedgaonkar, G.S.; Sridevi, J.P.; Jeankumar, V.U.; Saxena, S.; Devi, P.B.; Renuka, J.; Yogeewari, P.; Sriram, D. Development of 2-(4-oxoquinazolin-3(4H)-yl)acetamide derivatives as novel enoyl-acyl carrier protein reductase (InhA) inhibitors for the treatment of tuberculosis. *Eur. J. Med. Chem.* **2014**, *86*, 613–627. [[CrossRef](#)]
29. Kumar, A.; Kumari, N.; Bhattacharjee, S.; Venugopal, U.; Parwez, S.; Siddiqi, M.I.; Krishnan, M.Y.; Panda, G. Design, synthesis and biological evaluation of (Quinazoline 4-yloxy)acetamide and (4-oxoquinazoline-3(4H)-yl)acetamide derivatives as inhibitors of Mycobacterium tuberculosis bd oxidase. *Eur. J. Med. Chem.* **2022**, *242*, 114639. [[CrossRef](#)]
30. AbdElhameid, M.K.; Labib, M.B.; Negmeldin, A.T.; Al-Shorbagy, M.; Mohammed, M.R. Design, synthesis, and screening of ortho-amino thiophene carboxamide derivatives on hepatocellular carcinomas VEGFR-2 Inhibitors. *J. Enzym. Inhib. Med. Chem.* **2018**, *33*, 1472–1493. [[CrossRef](#)]
31. Remes, C.; Paun, A.; Zarafu, I.; M Tudose, M.; Caproiu, M.T.; Ionita, G.; Bleotu, C.; Matei, L.; Ionita, P. Chemical and biological evaluation of some new antipyrine derivatives with particular properties. *Bioorg. Chem.* **2012**, *41–42*, 6–12. [[CrossRef](#)]
32. Bem, M.; Baratoiu, R.; Radutiu, C.; Lete, C.; Mocanu, S.; Ionita, G.; Lupu, S.; Caproiu, M.T.; Madalan, A.M.; Patrascu, B.; et al. Synthesis and structural characterization of some novel methoxyamino derivatives with acid-basa and redox behavior. *J. Mol. Struct.* **2018**, *1173*, 291–299. [[CrossRef](#)]
33. Paun, A.; Zarafu, I.; Caproiu, M.T.; Draghici, C.; Maganu, M.; Ionita, P.; Cotar, A.I.; Chifiriuc, M.C. Synthesis and evaluation of several benzocaine derivatives. *C. R. Chim.* **2013**, *16*, 665–671. [[CrossRef](#)]
34. Molecular Operating Environment (MOE). 2022.02 Chemical Computing Group ULC, 1010 Sherbooke St. West, Suite #910, Montreal, QC, Canada, H3A 2R7. 2022. Available online: https://www.chemcomp.com/Research-Citing_MOE.htm (accessed on 30 March 2023).
35. Berman, H.M.; Westbrook, J.; Feng, Z.; Gilliland, G.; Bhat, T.N.; Weissig, H.; Shindyalov, I.N.; Bourne, P.E. The Protein Data Bank. *Nucleic Acids Res.* **2000**, *28*, 235–242. [[CrossRef](#)] [[PubMed](#)]
36. Binda, C.; Newton-Vinson, P.; Hubálek, F.; Edmondson, D.E.; Mattevi, A. Structure of Human Monoamine Oxidase B, a Drug Target for the Treatment of Neurological Disorders. *Nat. Struct. Biol.* **2002**, *9*, 22–26. [[CrossRef](#)] [[PubMed](#)]
37. Orlando, B.J.; Malkowski, M.G. Crystal Structure of Rofecoxib Bound to Human Cyclooxygenase-2. *Acta Crystallogr. F Struct. Biol. Commun.* **2016**, *72*, 772–776. [[CrossRef](#)]
38. Müller, C.W.; Rey, F.A.; Sodeoka, M.; Verdine, G.L.; Harrison, S.C. Structure of the NF-KB P50 Homodimer Bound to DNA. *Nature* **1995**, *373*, 311–317. [[CrossRef](#)]
39. Udrea, A.-M.; Dinache, A.; Staicu, A.; Avram, S. Target Prediction of 5,10,15,20-Tetrakis(4'-Sulfonatophenyl)-Porphyrin Using Molecular Docking. *Pharmaceutics* **2022**, *14*, 2390. [[CrossRef](#)]
40. Dumitrascu, F.; Udrea, A.-M.; Caira, M.R.; Nuta, D.C.; Limban, C.; Chifiriuc, M.C.; Popa, M.; Bleotu, C.; Hanganu, A.; Dumitrascu, D.; et al. In Silico and Experimental Investigation of the Biological Potential of Some Recently Developed Carprofen Derivatives. *Molecules* **2022**, *27*, 2722. [[CrossRef](#)]
41. Bordei, A.T.; Nuta, D.C.; Căproiu, M.T.; Dumitrascu, F.; Zarafu, I.; Ioniță, P.; Bădiceanu, C.D.; Avram, S.; Chifiriuc, M.C.; Bleotu, C.; et al. Design, Synthesis and In Vitro Characterization of Novel Antimicrobial Agents Based on 6-Chloro-9H-carbazol Derivatives and 1,3,4-Oxadiazole Scaffolds. *Molecules* **2020**, *25*, 266. [[CrossRef](#)]
42. Buiiu, C.; Putz, M.V.; Avram, S. Learning the Relationship between the Primary Structure of HIV Envelope Glycoproteins and Neutralization Activity of Particular Antibodies by Using Artificial Neural Networks. *Int. J. Mol. Sci.* **2016**, *17*, 1710. [[CrossRef](#)]
43. Morris, G.M.; Huey, R.; Olson, A.J. Using AutoDock for Ligand-Receptor Docking. *Curr. Protoc. Bioinform.* **2008**, *24*, 8.14.1–8.14.40. [[CrossRef](#)] [[PubMed](#)]
44. Udrea, A.-M.; Dinache, A.; Pagès, J.-M.; Pirvulescu, R.A. Quinazoline Derivatives Designed as Efflux Pump Inhibitors: Molecular Modeling and Spectroscopic Studies. *Molecules* **2021**, *26*, 2374. [[CrossRef](#)] [[PubMed](#)]
45. Nistorescu, S.; GradisteanuPircalabioru, G.; Udrea, A.-M.; Simon, A.; Pascu, M.L.; Chifiriuc, M.-C. Laser-Irradiated Chlorpromazine as a Potent Anti-Biofilm Agent for Coating of Biomedical Devices. *Coatings* **2020**, *10*, 1230. [[CrossRef](#)]
46. Vlaicu, I.D.; Olar, R.; Maxim, C.; Chifiriuc, M.C.; Bleotu, C.; Stănică, N.; Scăețeanu, G.V.; Dulea, C.; Avram, S.; Badea, M. Evaluating the biological potential of some new cobalt (II) complexes with acrylate and benzimidazole derivatives. *Appl. Org. Chem.* **2019**, *33*, e4976. [[CrossRef](#)]
47. pkCSM: Predicting Small-Molecule Pharmacokinetic Properties using Graph-Based Signatures. Available online: <https://biosig.lab.uq.edu.au/pkcsm/> (accessed on 30 March 2023).
48. Avram, S.; Mernea, M.; Bagci, E.; Hritcu, L.; Borcan, L.C.; Mihailescu, D.F. Advanced Structure-activity Relationships Applied to *Mentha spicata* L. Subsp. *spicata* Essential Oil Compounds as AChE and NMDA Ligands, in Comparison with Donepezil, Galantamine and Memantine—New Approach in Brain Disorders Pharmacology. *CNS Neurol. Disord. Drug Targets.* **2017**, *16*, 800–811. [[CrossRef](#)] [[PubMed](#)]
49. Gallo, K.; Goede, A.; Preissner, R.; Gohlke, B.-O. SuperPred 3.0: Drug classification and target prediction—a machine learning approach. *Nucleic Acids Res.* **2022**, *50*, W726–W731. [[CrossRef](#)] [[PubMed](#)]

50. Mohi-Ud-Din, R.; Mir, R.H.; Sawhney, G.; Dar, M.A.; Bhat, Z.A. Possible Pathways of Hepatotoxicity Caused by Chemical Agents. *Curr. Drug Metab.* **2019**, *20*, 867–879. [[CrossRef](#)] [[PubMed](#)]
51. Berechet, A. Cercetări în seria 4-chinazolonei. Nota 1. Sinteza uretanilor N-[2-metil-4-ceto-chinazolinil(3)metal] O-substituiti cu radical alchil. *Farmacia* **1967**, *15*, 287–290.

Disclaimer/Publisher's Note: The statements, opinions and data contained in all publications are solely those of the individual author(s) and contributor(s) and not of MDPI and/or the editor(s). MDPI and/or the editor(s) disclaim responsibility for any injury to people or property resulting from any ideas, methods, instructions or products referred to in the content.